THE JOURNAL OF BIOLOGICAL CHEMISTRY VOL. 290, NO. 27, pp. 16463–16476, July 3, 2015

Factor VIII Interacts with the Endocytic Receptor Low-density Lipoprotein Receptor-related Protein 1 via an Extended Surface Comprising "Hot-Spot" Lysine Residues◆

Received for publication, March 11, 2015, and in revised form, April 8, 2015 Published, JBC Papers in Press, April 21, 2015, DOI 10.1074/jbc.M115.650911

Maartje van den Biggelaar[‡1], Jesper J. Madsen[§], Johan H. Faber[§], Marleen G. Zuurveld[‡], Carmen van der Zwaan[‡], Ole H. Olsen[§], Henning R. Stennicke[§], Koen Mertens[‡¶], and Alexander B. Meijer[‡¶]

From the [‡]Department of Plasma Proteins, Sanquin Blood Supply Foundation, 1066 CX Amsterdam, The Netherlands, [§]Global Research, Novo Nordisk A/S, DK-2760 Måløv, Denmark, and the [¶]Department of Pharmaceutics, Utrecht Institute for Pharmaceutical Sciences, Utrecht University, 3508 TC Utrecht, The Netherlands

Background: It is unclear how the LDL receptor family binds large protein ligands.
Results: HDX and lysine scanning identified factor (F)VIII regions and specific lysine residues binding low-density lipoprotein receptor-related protein 1 (LRP1).
Conclusion: FVIII-LRP1 interaction involves multiple "hot-spot" lysine residues in the A3C1 domains.
Significance: Our study sheds light on interactions of complex ligands with the LDL receptor family.

Lysine residues are implicated in driving the ligand binding to the LDL receptor family. However, it has remained unclear how specificity is regulated. Using coagulation factor VIII as a model ligand, we now study the contribution of individual lysine residues in the interaction with the largest member of the LDL receptor family, low-density lipoprotein receptor-related protein (LRP1). Using hydrogen-deuterium exchange mass spectrometry (HDX-MS) and SPR interaction analysis on a library of lysine replacement variants as two independent approaches, we demonstrate that the interaction between factor VIII (FVIII) and LRP1 occurs over an extended surface containing multiple lysine residues. None of the individual lysine residues account completely for LRP1 binding, suggesting an additive binding model. Together with structural docking studies, our data suggest that FVIII interacts with LRP1 via an extended surface of multiple lysine residues that starts at the bottom of the C1 domain and winds around the FVIII molecule.

The low-density lipoprotein receptor family is an ancient family of transmembrane receptors regulating diverse biological processes ranging from lipoprotein metabolism to blood coagulation (1–3). Members of the LDL receptor family are able to interact with an unusual number of ligands; *e.g.* more than 30 ligands have been reported for the largest member, LRP1,[2] including lipoproteins, viruses, bacteria toxins, proteinase-inhibitor complexes, and coagulation proteins (4, 5). Given the importance of the LDL receptor family in human physiology, much research has been focused on the questions of how the various members of the LDL receptor family can interact with such a large variety of structurally unrelated ligands and which molecular mechanisms regulate specificity of the interaction.

The LDL receptor family is characterized by the presence of a varying number of distinct domains: the YWTD β-propeller and EGF domains, a transmembrane region, an intracellular cytoplasmic tail, and ligand-binding domains or complement-type repeats (CR domains). Ligand binding is mediated by clusters of structured CR domains that consist of ~40 amino acids folding into a compact structure. Each CR domain contains three disulfide bonds, a highly conserved octahedral calcium-binding cage, and a short β-hairpin near the N-terminal end (6). The calcium cage is required both for structural integrity of the CR domain as well as for direct ligand binding and is formed by six oxygen atoms derived from four conserved acidic residues and two backbone carbonyl groups (6–9). The CR domains are connected by flexible linker sequences, thereby enabling the receptor family to bind to a wide range of proteins.

Most of our knowledge on ligand-receptor interaction is based on the intracellular chaperone receptor-associated protein (RAP), which binds with high affinity to members of the LDL receptor family (10, 11). Based on a co-crystallization study of two CR domains from the LDL receptor with the third domain of RAP (RAP-D3), a general mode for ligand recognition by lipoprotein receptors has been proposed (12). In this "acidic necklace" model, each CR domain encircles an ϵ-amino group of a lysine residue in a tripartite salt bridge (Lys^{256} and Lys^{270} in RAP-D3) via the three remaining oxygen atoms from the acidic residues forming the octahedral calcium cage (12). This model was supported by a previous study in which Lys^{256} and Lys^{270} were identified as being critical for the interaction of RAP-D3 to complete LRP1 using random mutagenesis (13). Further support for the lysine binding model was provided by the NMR structure of the complex of complement-type repeat 5 and 6 of LRP1 and the first domain of RAP (RAP-D1) (14), although the models differ in terms of the additional contribution of hydrophobic interactions. Recently, we further experi-

◆ This article was selected as a Paper of the Week.

[1] To whom correspondence should be addressed: Dept. of Plasma Proteins, Sanquin Research, Plesmanlaan 125, 1066 CX Amsterdam, The Netherlands. Tel.: 31-20-5121289; Fax: 31-20-5123310; E-mail: m.vandenbiggelaar@sanquin.nl.

[2] The abbreviations used are: LRP, low-density lipoprotein receptor-related protein; HDX, hydrogen-deuterium exchange; RAP, receptor-associated protein; FVIII, factor VIII; CR, complement-type repeat; LDLR, low density lipoprotein receptor.

mentally demonstrated that positively charged arginines cannot substitute for the two dominant lysine residues (Lys^{256} and Lys^{270}) in the interaction with the RAP-D3 domain and LRP1 (15). In agreement with these data, arginine residues also do not take over lysine residues in the high-affinity interactions of RAP-D1 (Lys^{143} and Lys^{146}) with the LDL receptor (16). In a recent elegant study, Dolmer *et al.* (17) established that lysine residues are the sole contributors to binding of RAP-D3 to an LRP1 fragment containing two CR domains and that pairs of lysine residues ensure high-affinity interaction in an additive rather than a synergistic manner.

RAP prevents premature ligand binding during biosynthesis of the LDL receptor family members by efficiently competing with other ligands (18–20). It therefore seems very possible that the affinity and molecular mechanism of interaction have been optimized during evolution. Although the acidic necklace model is consistent with previous observations that lysine residues are implicated in the binding of ligands other than RAP to the LDL receptor family (21–28), it has remained unclear how large ligands containing multiple lysine residues interact with the LDL receptor family members. This is particularly relevant because experiments using single CR domains and simple (modified) amino acids have also shown that arginine and protonated histidine, especially pairs of proximal charges, can interact well with CR domains (29). Taken together, it has also remained unclear whether lysine residues make a dominant contribution to the interaction with the LDL receptor family for low-affinity ligands. Another important question is how specificity of the interaction is attained. It has been suggested that high-affinity interaction requires the engagement of at least two separate lysine residues located at an appropriate distance from each other (12, 30). In addition, it has been proposed that there are modest requirements for being a coordinating lysine residue and that specificity may be regulated by a second, immediately adjacent positive charge (17, 29). We therefore set out to study in detail the interaction of LRP1 with its low-affinity ligand FVIII using two independent approaches with particular emphasis on lysine residues. Hydrogen-deuterium mass spectrometry was used to obtain insight in the contact areas on B-domain-deleted FVIII for LRP1 cluster II. In addition, we used a lysine mutagenesis approach to study the specific role of lysine residues in the FVIII light chain in the interaction with full-length LRP1 and LRP1 cluster II. These combined studies reveal important novel aspects of the interaction between FVIII and LRP1.

Experimental Procedures

Plasmid Mutagenesis—FVIII light chain in pcDNA3.1 was created from wild type FVIII-GFP in pcDNA3.1 (31) by fusing the signal peptide to the acidic *a3* domain (glutamic acid at position 1649) by QuikChange™ mutagenesis (Stratagene, La Jolla, CA) using forward primer 5′-TTGCGATTCTGCTTTAGTGAAATAACTCGTACTACT-3′ and reverse primer 5′-AGTAGTACGAGTTATTTCACTAAAGCAGAATCGCAA-3′. B domain-deleted (del 746–1639) factor VIII (FVIIIdB) in pcDNA3.1 has been described before (32). Point mutations in the FVIII light chain and FVIIIdB were introduced by QuikChange™ mutagenesis (Stratagene) using the appropriate primers. The coding regions of all constructs were verified by sequence analysis. Sequence reactions were performed with BigDye terminator sequencing kit (Applied Biosystems, Foster City, CA).

Expression of Recombinant Proteins—Recombinant factor VIII (FVIII) Turoctocog alfa (previously named N8) was produced in CHO cells as described previously (33). The molecule consists of a heavy chain of 88 kDa including a 21-amino acid residue truncated B-domain and a light chain of 79 kDa; it contains four *N*-glycosylation sites of which two are complex biantennary glycans and two are high-mannose structures. FVIII light chain variants were expressed under serum-free conditions using 293-F cells (Invitrogen, R790-07) and FreeStyle 293 expression medium (Invitrogen). Freestyle 293 cells were transfected using 293fectin (Invitrogen) according to the manufacturer's instructions for small scale expression and using linear PEI M_r ~25,000 (Polysciences Inc.) for large scale expression. Cells were harvested 4–5 days after transfection. Cells were centrifuged for 8 min at 4600 × *g*, and the supernatant was collected. The cell pellet was subsequently washed with 0.55 M NaCl in FreeStyle 293 expression medium and centrifuged for 8 min at 4600 × *g*. The conditioned medium was combined with the 0.55 M NaCl wash and filtered using a 0.22-μm disposable filter unit. FVIII light chain variants were purified using CLB-CAg117 coupled to CNBr-Sepharose 4B as an affinity matrix followed by concentration using Q-Sepharose (31) (Amersham Biosciences, Roosendaal, The Netherlands). HEK293 cell lines stably expressing FVIIIdB variants were produced as described (34) and grown in DMEM-F12 medium supplemented with 10% FCS. Recombinant FVIIIdB variants were purified and analyzed as described using CLB-VK34 IgG1 coupled to CNBr-Sepharose 4B as an affinity matrix followed by concentration using Q-Sepharose (21). LRP1 cluster II was expressed in baby hamster kidney cells and purified as described (35) using glutathione *S*-transferase fused RAP coupled to CNBr-Sepharose 4B as an affinity matrix. Subsequently, purified LRP1 cluster II was concentrated using Q-Sepharose.

HDX-MS Experiments—189 μM FVIII and 256 μM LRP1 cluster II were dialyzed to a buffer comprising 20 mM imidazole, pH 7.3, 10 mM $CaCl_2$, 500 mM NaCl, and complex formation was allowed for 30 min at room temperature. In-exchange of deuterium was initiated by a 10-fold dilution into either 20 mM imidazole, pH 7.3, 10 mM $CaCl_2$, 111 mM NaCl in 100% H_2O for the undeuterated experiments or 20 mM imidazole, pD 7.3, 10 mM $CaCl_2$, 111 mM NaCl in 100% D_2O for the deuterated experiments. All sample deuterium labeling, quenching, injection to MS, and timing of samples were handled by an automated setup (Leap Technologies Inc.) as described (36) with minor adjustments. Minor modifications included exchange times ranging from 10 s to 256 min, the use of a 7-min linear acetonitrile gradient of 8–45% containing 0.1% formic acid, and the use of a SYNAPT G2 high definition mass spectrometer (Waters). Four undeuterated and two complete HDX experiments were performed for FVIII and FVIII in complex with LRP1 cluster II within 2 consecutive days. Blank injections were performed between each sample injection to confirm the absence of peptide carryover from previous runs. Peptic peptides were identified in separate experiments using MS^E methods. MS^E data

were processed using ProteinLynx Global Server software (Waters version 2.4). Searches of MS^E data were conducted as nonspecific digest with N-terminal acetylation of FVIII as modification. The sequence coverage map of FVIII was plotted using the online tool MSTools (37). The relative deuterium incorporation levels for each peptic peptide were automatically calculated using DynamX software (Waters) as described (36). The data were expressed in either mass units (Da) or relative fractional exchange, which was calculated by dividing the deuterium level (in Da) by the total number of backbone amide hydrogens that could have become deuterated (equal to the number of amino acids, minus proline residues minus 1 for the N-terminal amide). The experimental uncertainty of measuring a deuterium level was found to be ±0.15 Da. Using this value of experimental uncertainty and a 98% confidence interval, a significant difference value of 0.5 Da was calculated for individual time points, and a value of 1.5 kDa was calculated for summed HDX differences across all time points.

Surface Plasmon Resonance Analysis—Association and dissociation of LRP1 cluster II to FVIII light chain and FVIIIdB variants were assessed by SPR analysis employing a BIAcore 3000 biosensor (Biacore AB, Uppsala, Sweden). The anti-C2 antibody CLB-EL14 IgG4 (38) (26 fmol/mm^{-2} for FVIII light chain variants and 39 fmol/mm^{-2} for FVIIIdB variants) was immobilized onto a CM5 sensor chip using the amine coupling method according to the manufacturer's instructions. Subsequently, FVIII light chain variants were bound directly from medium to the anti-C2 antibody at a density of 17 fmol/mm^{-2}, and purified FVIIIdB variants were bound at a density of 9 fmol/mm^{-2}. LRP1 cluster II (0.2–200 nM) was passed over the FVIII light chain or FVIIIdB variants in a buffer containing 150 mM NaCl, 5 mM $CaCl_2$, 0.005% (v/v) Tween 20, and 20 mM Hepes (pH 7.4) at 25 °C with a flow rate of 20 μl/min. The sensor chip surface was regenerated three times after each concentration of LRP1 cluster II using the same buffer containing 1 M NaCl. Binding to FVIII light chain or FVIIIdB variants was corrected for binding in the absence of FVIII. Binding data during the association phase were fitted in a one-phase exponential association model. Responses at equilibrium were plotted as a function of the LRP1 cluster II concentration. The responses at equilibrium were fitted by non-linear regression using a standard hyperbola to generate K_D values assuming similar B_{max} values (GraphPad Prism 4 software, San Diego, CA). To study the contribution of lysine residues on the interaction between LRP1 cluster II and the FVIII light chain, lysine residues were modified by passing over 50 mM sulfo-NHS acetate or sulfo-NHS biotin (Thermo Fisher Scientific) for 10 min at 25 °C with a flow rate of 20 μl/min prior to passing over LRP1 cluster II (0.2–200 nM) and anti-*a3* antibody CLB-CAg69 (39) (0.1–100 nM). Binding of purified FVIII light chain and FVIIIdB variants to full-length LRP1 was studied by coupling LRP1 (Biomac, Leipzig, Germany) directly on a CM5 chip according to the manufacturer's instructions at three different densities (15, 18, and 21 fmol/mm^{-2}). FVIII light chain variants (1–25 μg/ml based on Bradford analysis) and FVIIIdB variants (5–1000 units/ml based on chromogenic activity) were passed over the immobilized LRP1 in a buffer containing 150 mM NaCl, 5 mM $CaCl_2$, 0.005% (v/v) Tween 20, and 20 mM Hepes (pH 7.4) at

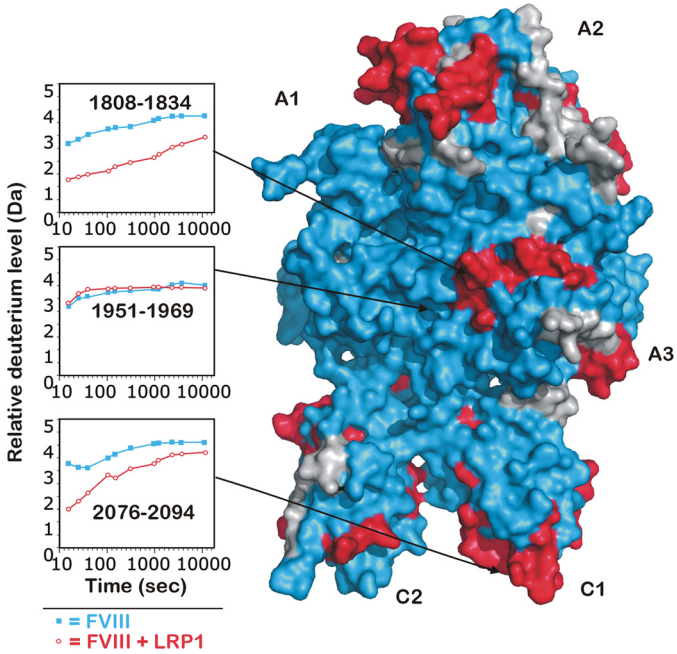

FIGURE 1. **HDX of FVIII and FVIII incubated with LRP1 cluster II monitored by mass spectrometry.** Surface plot of FVIII based on the crystal structure of FVIII (Protein Data Bank code 4BDV) is shown. Peptides that display reduced deuterium incorporation (>2 S:D) following complex formation with LRP1 are colored in *red*, and peptides that displayed no changes are colored in *blue*. Areas uncovered by the peptide fragment are *gray*. *Inset*: fitted HDX curves of the representative peptides of FVIII (*blue*) and FVIII incubated with LRP1 cluster II (*red*) are shown, with raw data indicated by *solid squares* and *open circles*.

25 °C with a flow rate of 20 μl/min. The sensor chip surface was regenerated three times after each concentration of FVIII using the same buffer containing 1 M NaCl. Binding to LRP1 was corrected for binding in the absence of LRP1. The response units at time point 235 s were plotted as a function of the concentration.

Structural Modeling—The illustrative model of the triplet canonical binding mode of LRP to the light chain of FVIII is constructed using the Rosetta modeling suite (40) and the NAMD molecular dynamics software package (41). Based on structural alignment with the x-ray crystallographic structure of the LDLR-RAP complex (Protein Data Bank (PDB): 2FCW) (12), a homology model of the calcium-loaded LRP double CR 56 was created using the Rosetta comparative modeling protocol (42) by generating 30,000 decoys of the LRP1 CR56 double module. Calcium ions, one per complementary repeat, were inserted based on the structural alignments and adjusted slightly by hand to remove atomistic overlap. The resulting calcium-loaded LRP double complementary repeat 56 (LRP1 CR56) model was positioned relative to the light chain of FVIII (PDB: 4BDV, chain B) (43) to reconstruct the interaction motif of the LDLR-RAP complex in which CR5 interacts with Lys^{2065} and CR6 interacts with Lys^{2092}. The lysine residues of the FVIII light chain, Lys^{2065} and Lys^{2092}, were overlaid with the NZ atoms of the two interacting lysine residues (Lys^{256} and Lys^{270}) of RAP. To complete the triplet binding mode, a further CR5 module was positioned to interact with Lys^{2136} and connected to its adjacent CR56 module by the loop modeling application in Rosetta, making 1,000 loop decoys. The specific sequence to be remodeled in each fragment was identified using the domain

linker predictor DLP-SVM (44). The sequence for a CR56-CR56 chain was analyzed using their SVM-Joint consolidated predictor, which identified region CSHSARTCPPNQFSCASG-RCIPI (residues 80–102 according to LRP alignment numbering) as a possible inter-domain linker. Because the natural chain break is after position 82 and both Cys^{80} and Cys^{87} are involved in forming intra-module disulfide bonds, we chose to limit the remodel region to residues 80–87. The resulting LRP1 CR565-FVIII light chain model in which the interaction pattern is CR565 against Lys^{2065}-Lys^{2092}-Lys^{2136} is truncated to remove the a3A3 and C2 domains of the FVIII light chain, leaving only the C1 domain (chain B residues 2020–2171). This system was solvated with ~10,000 TIP3P water molecules and ionized to salt concentration of 0.15. Following an energy minimization for 5,000 steps by a steepest decent method, the system was equilibrated using molecular dynamics simulations with constant number of atoms (n), constant pressure ($P = 1$ atm), and constant temperature ($T = 310$ K) for 5 ns, allowing it to settle.

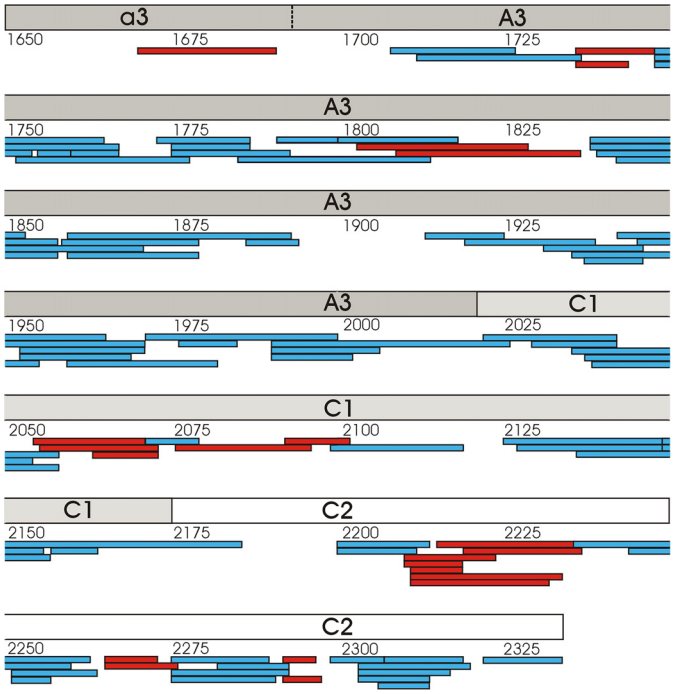

FIGURE 2. **HDX of FVIII and FVIII in complex with LRP1 cluster II monitored by mass spectrometry.** Sequence coverage of peptide fragments of LC FVIII is shown. Peptides that display reduced deuterium incorporation (>2 S:D) following complex formation with LRP1 are colored in *red*, and peptides that displayed no changes are colored in *blue*. Domains of LC FVIII are shown schematically.

Results

HDX-MS of LRP1 Interaction with Cofactor FVIII—We have previously established that the main LRP1 binding on FVIII is localized in the FVIII light chain (45). HDX mass spectrometry was now employed to elucidate the surface areas on FVIII that show reduced HDX in the presence of LRP1 cluster II. These areas either are covered by complement-type repeats or exhibit a local change in conformation caused by cluster II binding. HDX of FVIII in the presence and absence of LRP1 cluster II was followed at various time intervals ranging from 10 s to 256 min. Inline pepsin protein digest conditions were established that afforded peptides of reasonably small length (typically 5–20 amino acids). These conditions enabled detection of a total of 277 peptides covering 76% of the primary sequence of FVIII, with redundant coverage of all subunits, *i.e.* A1, A2, A3, C1, and C2 (Figs. 1 and 2). The majority of the peptides displayed an exchange pattern that is unaffected by the binding of LRP1 cluster II (Figs. 1 and 2, *blue color*). However, several overlapping peptic peptide fragments encompassing residues 114–132, 369–387, 399–428, 481–506, 1669–1689, 1735–1746, 1817–1834, 2054–2069, 2078–2097, 2213–2234, 2264–2273, and 2292–2296 showed reduced HDX in the presence of LRP1 cluster II (Figs. 1 and 2, *red color*). The raw data of some representative HDX profiles for these peptides are shown in Fig. 1. This analysis revealed that the regions that demonstrate reduced HDX are predominantly on the FVIII light chain and are scattered throughout the *a3*, A3, C1, and C2 domains (Figs. 1 and 2).

Chemical Modification of Lysine Residues in the FVIII Light Chain Abolishes the Interaction with LRP1 Cluster II—To address the role of lysine residues in the interaction between LRP1 cluster II and the FVIII light chain, we chemically modified lysine residues of the FVIII light chain on an SPR sensor

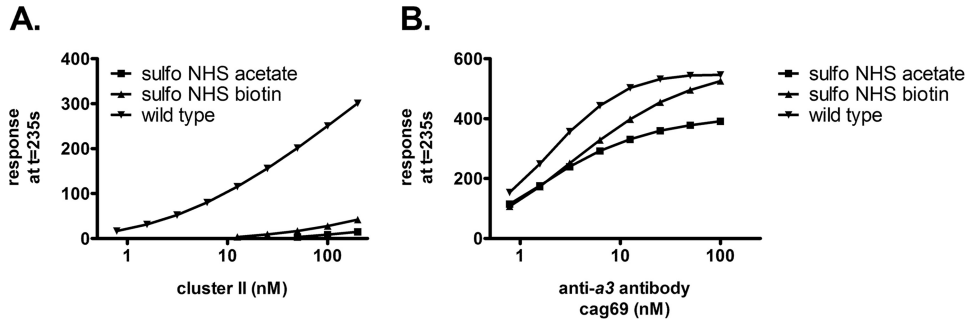

FIGURE 3. **Chemical modification of lysine residues in the FVIII light chain abolishes the interaction with LRP1 cluster II.** Association and dissociation of LRP1 cluster II to FVIII light chain were assessed by SPR analysis employing a BIAcore 3000 biosensor (Biacore AB). The anti-C2 antibody CLB-EL14 IgG4 (26 fmol/mm^{-2}) was immobilized onto a CM5 sensor chip using the amine coupling method according to the manufacturer's instructions. Subsequently, FVIII light chain was bound to the anti-C2 antibody at a density of 17 fmol/mm^{-2}. To study the contribution of lysine residues on the interaction between LRP1 cluster II and the FVIII light chain, lysine residues were modified by passing over 50 mM sulfo-NHS acetate or sulfo-NHS biotin (Thermo Fisher Scientific) for 10 min at 25 °C with a flow rate of 20 μl/min. *A* and *B*, LRP1 cluster II (0.2–200 nM) (*A*) and anti-*a3* antibody CLB-CAg69 (0.1–100 nM) (*B*) were passed over the FVIII light chain in a buffer containing 150 mM NaCl, 5 mM $CaCl_2$, 0.005% (v/v) Tween 20, and 20 mM Hepes (pH 7.4) at 25 °C with a flow rate of 20 μl/min. The sensor chip surface was regenerated three times after each concentration of LRP1 cluster II using the same buffer containing 1 M NaCl. Binding to FVIII light chain was corrected for binding in the absence of FVIII. The response at 235 s after association is plotted as a function of the concentration.

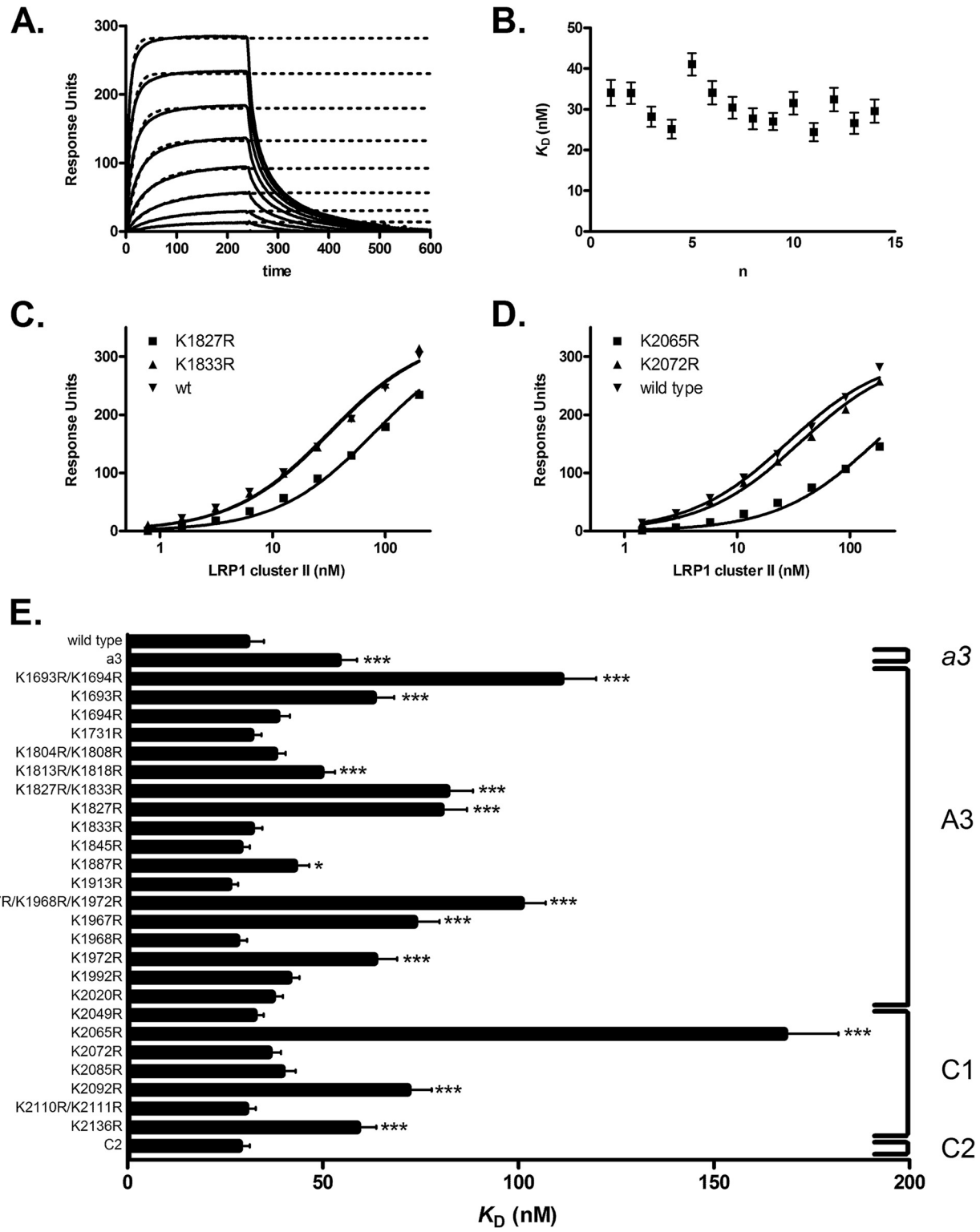

FIGURE 4. **Library of lysine to arginine replacements in the FVIII light chain identifies the contribution of multiple lysine residues in the interaction with LRP1 cluster II.** Association and dissociation of LRP1 cluster II to FVIII light chain variants were assessed by SPR analysis employing a BIAcore 3000 biosensor (Biacore AB). The anti-C2 antibody CLB-EL14 IgG4 (26 fmol/mm^{-2}) was immobilized onto a CM5 sensor chip using the amine coupling method according to the manufacturer's instructions. Subsequently, FVIII light chain variants were bound to the anti-C2 antibody at a density of 17 fmol/mm^{-2}. LRP1 cluster II (0.2–200 nM) was passed over the FVIII light chain variants in a buffer containing 150 mM NaCl, 5 mM $CaCl_2$, 0.005% (v/v) Tween 20, and 20 mM Hepes (pH 7.4) at 25 °C with a flow rate of 20 μl/min. The sensor chip surface was regenerated three times after each concentration of LRP1 cluster II using the same buffer containing 1 M NaCl. Binding to FVIII light chain variants was corrected for binding in the absence of FVIII. Binding data during the association phase were fitted in a one-phase exponential association model. *A*, representative experiment for the interaction between LRP1 cluster II and wild type FVIII light chain. *B*, on each SPR sensor chip, we included a control channel (only CLB-EL14 IgG4), wild type FVIII light chain, and two FVIII light chain variants. Therefore, wild type FVIII light chain was analyzed multiple times ($n = 14$) *C* and *D*, representative experiments for variants. *E*, the K_D for LRP1 cluster II for the FVIII light chain variants was compared with the K_D of wild type FVIII light chain ($n = 14$, degrees of freedom = 13, *, $p < 0.10$, t value = 2.16, ***, $p < 0.001$, t value = 4.22) using a two-tailed Student's t test. *Error bars* indicate ± S.D.

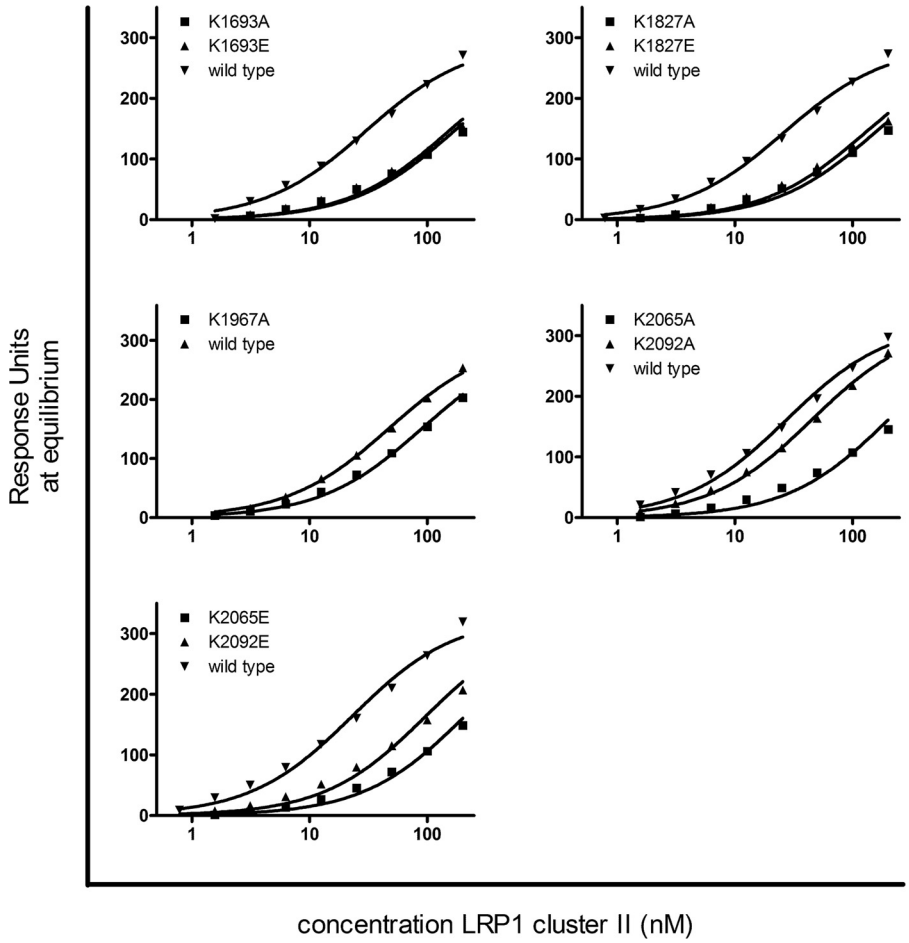

FIGURE 5. **Lysine to alanine and lysine to glutamic acid replacements at position 1693, 1827, 1967, 2065, and 2092.** Association and dissociation of LRP1 cluster II to FVIII light chain variants Lys^{1693}, Lys^{1827}, Lys^{1967}, Lys^{2065}, and Lys^{2092} were assessed by SPR analysis employing a BIAcore 3000 biosensor (Biacore AB). The anti-C2 antibody CLB-EL14 IgG4 (26 fmol/mm^{-2}) was immobilized onto a CM5 sensor chip using the amine coupling method according to the manufacturer's instructions. Subsequently, FVIII light chain variants were bound to the anti-C2 antibody at a density of 17 fmol/mm^{-2}. LRP1 cluster II (0.2–200 nM) was passed over the FVIII light chain variants in a buffer containing 150 mM NaCl, 5 mM $CaCl_2$, 0.005% (v/v) Tween 20, and 20 mM Hepes (pH 7.4) at 25 °C with a flow rate of 20 μl/min. The sensor chip surface was regenerated three times after each concentration of LRP1 cluster II using the same buffer containing 1 M NaCl. Binding to FVIII light chain variants was corrected for binding in the absence of FVIII. Binding data during the association phase were fitted in a one-phase exponential association model.

TABLE 1

Effect of replacement of lysine residues by positively charged arginine, uncharged alanine, or negatively charged glutamic acid on the interaction between the FVIII light chain and LRP1 cluster II

Association and dissociation of LRP1 cluster II to FVIII light chain variants Lys-1693, Lys-1827, Lys-1967, Lys-2065, and Lys-2092 was assessed by SPR analysis employing a BIAcore 3000 biosensor (Biacore AB, Uppsala, Sweden). The anti-C2 antibody CLB-EL14 IgG4 (26 fmol/mm^{-2}) was immobilized onto a CM5 sensor chip using the amine coupling method according to the manufacturer's instructions. Subsequently, FVIII light chain variants were bound to the anti-C2 antibody at a density of 17 fmol/mm^{-2}. LRP1 cluster II (0.2–200 nM) was passed over the FVIII light chain variants in a buffer containing 150 mM NaCl, 5 mM $CaCl_2$, 0.005% (v/v) Tween 20, and 20 mM Hepes (pH 7.4) at 25 °C with a flow rate of 20 μl/min. The sensor chip surface was regenerated three times after each concentration of LRP1 cluster II using the same buffer containing 1 M NaCl. Binding to FVIII light chain variants was corrected for binding in absence of FVIII. Binding data during the association phase were fitted in a one-phase exponential association model. ND, not determined.

Lysine position	Replacement		
	Arginine (K_D)	Alanine (K_D)	Glutamic acid (K_D)
	nM	nM	nM
1693	63 ± 5	170 ± 19	154 ± 17
1827	80 ± 7	157 ± 16	130 ± 13
1967	73 ± 6	91 ± 5	ND
2065	168 ± 14	202 ± 17	210 ± 22
2092	72 ± 6	45 ± 4	98 ± 10

chip using the compounds sulfo-NHS-acetate and sulfo-NHS-biotin. Both these compounds form stable, covalent amide bonds with primary amines, resulting in the replacement of the positively charged ϵ-amino group of the lysine residue by an uncharged acetate group (sulfo-NHS-acetate) or biotin group (sulfo-NHS-biotin). Subsequently, LRP1 cluster II and a control antibody CLB-CAg69 directed against the *a3* domain of FVIII were passed over the unmodified and chemically modified FVIII light chain. Although LRP1 cluster II readily bound to the unmodified FVIII light chain, no detectable binding was observed for the FVIII light chain in which the lysine residues were chemically modified (Fig. 3). As a control, the CLB-CAg69 antibody bound to a similar extent to the unmodified as well as to the chemically modified FVIII light chain (Fig. 3). These data suggest that lysine-containing surface patches mediate the interaction between LRP1 cluster II and the FVIII light chain.

Multiple Lysine Residues in the FVIII Light Chain Contribute to the Interaction with LRP1 Cluster II—To systematically address which lysine residues in the FVIII light chain contribute to LRP1 cluster II interaction, we constructed a library of FVIII variants carrying lysine to arginine (KR) replacements. All of

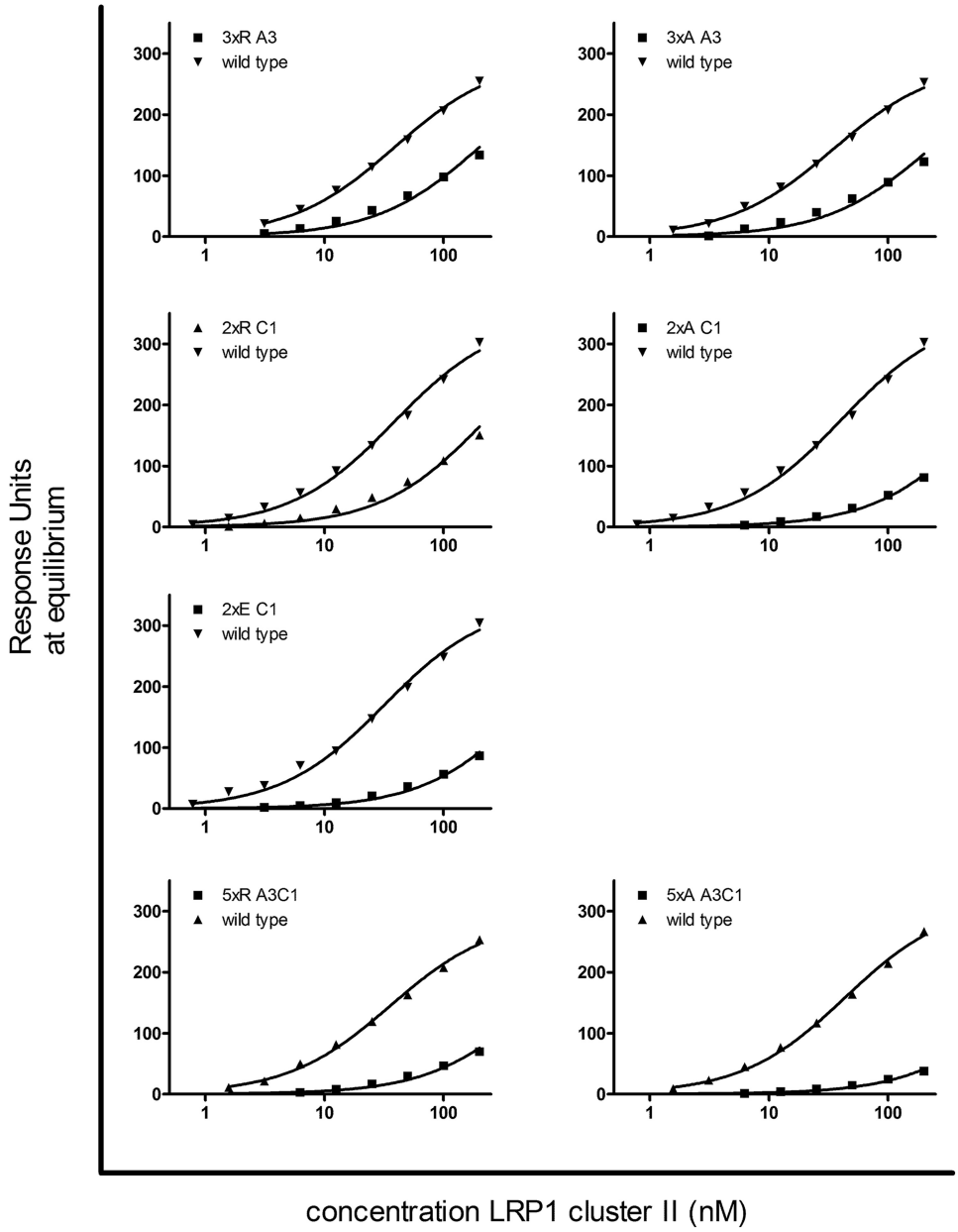

FIGURE 6. **Combined lysine replacements have an additive effect on LRP1 cluster II interaction.** Association and dissociation of LRP1 cluster II to FVIII light chain variants carrying replacements at positions Lys^{1693}, Lys^{1827}, and Lys^{1967} (A3), Lys^{2065} and Lys^{2092} (C1), and Lys^{1693}, Lys^{1827}, Lys^{1967}, Lys^{2065}, and Lys^{2092} (A3C1) were assessed by SPR analysis employing a BIAcore 3000 biosensor (Biacore AB). The anti-C2 antibody CLB-EL14 IgG4 (26 fmol/mm^{-2}) was immobilized onto a CM5 sensor chip using the amine coupling method according to the manufacturer's instructions. Subsequently, FVIII light chain variants were bound to the anti-C2 antibody at a density of 17 fmol/mm^{-2}. LRP1 cluster II (0.2–200 nM) was passed over the FVIII light chain variants in a buffer containing 150 mM NaCl, 5 mM $CaCl_2$, 0.005% (v/v) Tween 20, and 20 mM Hepes (pH 7.4) at 25 °C with a flow rate of 20 μl/min. The sensor chip surface was regenerated three times after each concentration of LRP1 cluster II using the same buffer containing 1 M NaCl. Binding to FVIII light chain variants was corrected for binding in the absence of FVIII. Binding data during the association phase were fitted in a one-phase exponential association model.

these variants were tested for LRP1 cluster II interaction using SPR analysis. On each SPR sensor chip, we included a control channel (only CLB-EL14 IgG4), wild type FVIII light chain, and two FVIII light chain variants. Therefore, wild type FVIII light chain was analyzed multiple times ($n = 14$). For each channel, binding data during the association phase were fitted in a one-phase exponential association model. A typical example of the binding curves as well as the fit of the one-phase exponential association model (*dotted line*) for wild type FVIII light chain is represented in Fig. 4*A*. Responses at equilibrium were plotted as a function of the LRP1 cluster II concentration and fitted by non-linear regression using a standard hyperbola to generate K_D values. The K_D value for wild type FVIII light chain was 30 ± 4 nM (Fig. 4*B*). Initially, we constructed FVIII light chain variants based on the domain structure of FVIII carrying 2 (*a3*), 17 (A3), 8 (C1), or 9 (C2) replacements. However, KR variants of the A3 domain (17 replacements) and the C1 domain (8 replacements) were poorly expressed. We therefore constructed KR variants carrying single, double, or triple lysine to arginine replacements in the A3 and C1 domain. Unfortunately, the K1732R FVIII light chain variant was poorly expressed and could not be assessed using SPR analysis. For all

of the other variants, binding to LRP1 cluster II was analyzed, and the K_D was calculated as described above. Representative experiments are shown in Fig. 4, *C* and *D*. The K_D for LRP1 cluster II for these variants was compared with the K_D of wild type (30 ± 4 nM) using a two-tailed Student's *t* test (Fig. 4*E*). Our SPR analysis showed that lysine residues in the C2 domain of the FVIII light chain do not contribute to the interaction with LRP1 cluster II. In contrast, multiple lysine residues in the *a3*A3C1 domains contributed to the interaction of FVIII to LRP1, although none of the individual substitutions completely abolished LRP1 cluster II binding. Lysine residues contributing to the interaction included Lys^{1673}/Lys^{1674}, Lys^{1693}, Lys^{1813}/Lys^{1818}, Lys^{1827}, Lys^{1967}, Lys^{1972}, Lys^{2065}, Lys^{2092}, and Lys^{2136} (Fig. 4*E*). Of these, Lys^{1693}, Lys^{1827}, and Lys^{1967} ranked the highest in the A3 domain, and Lys^{2065} and Lys^{2092} ranked the highest in the C1 domain. These residues were selected for further studies.

Single and Multiple Replacements of Selected Lysine Residues in the A3 Domain Lys^{1693}, Lys^{1827}, and Lys^{1967} and in the C1 Domain Lys^{2065} and Lys^{2092} by Arginine, Alanine, or Glutamic Acid—From the SPR data of our library of FVIII light chain variants, we concluded that multiple lysine residues contribute to the interaction with LRP1 cluster II. However, there are some lysine residues in the A3 domain (Lys^{1693}, Lys^{1827}, and Lys^{1967}) and in the C1 domain (Lys^{2065} and Lys^{2092}) that contribute most to the interaction. To study the effect of charge, these lysine residues were replaced by positively charged arginine, uncharged alanine, or negatively charged glutamic acid. The variant carrying a K1967E replacement was poorly expressed and could not be analyzed. All other FVIII light chain variants demonstrated a reduced interaction with LRP cluster II (Fig. 5 and Table 1), confirming the contribution of lysine residues at positions 1693, 1827, 1967, 2065, and 2092 to the interaction with LRP1 cluster II. There were no major differences in the interaction with LRP1 cluster II for FVIII light chain variants carrying lysine to arginine or lysine to alanine replacements for the positions 1967, 2065, and 2092. This confirms our previous observation that, despite their positive charge, arginine cannot replace lysine in the interaction with LRP1. However, for lysine residues at positions 1693 and 1827, alanine replacements demonstrated a higher K_D as compared with arginine replacements (Table 1), suggesting that although for these specific residues a lysine residue is preferred, the charge of the arginine can maintain some interaction with LRP1. In addition, we have reversed the positive charge of the lysine residue by replacing the lysine with a negatively charged glutamic acid residue. Alanine and glutamic acid variants demonstrated a similar K_D, indicating that there was no additive effect of neutralizing the charge (Table 1). To study the additive effect of combining lysine replacements, we constructed FVIII variants carrying 3 (Lys^{1693}, Lys^{1827}, and Lys^{1967}), 2 (Lys^{2065} and Lys^{2092}), and 5 lysine replacements. All FVIII light chain variants carrying the K1967E replacement were poorly expressed and could not be analyzed. All the other variants demonstrated a reduced interaction with LRP1 cluster II (Fig. 6 and Table 2). FVIII light chain variants containing 3 lysine replacements in the A3 domain demonstrated a slightly increased K_D as compared with the variants containing only 1 lysine replacement in the A3 domain. There was no major difference between the lysine to arginine and lysine to alanine variants (Table 2). For the C1 domain, the K_D for variants in which both Lys^{2065} and Lys^{2092} were replaced was increased as compared with the C1 variants carrying only 1 lysine replacement. For the C1 domain, alanine or glutamic acid replacements did result in a higher K_D as compared with arginine replacements (Table 2). The combined variants in which the 5 lysine residues in the A3 and C1 were replaced by arginine or alanine demonstrated a K_D that was ~20-fold (arginine) or 40-fold (alanine) reduced as compared with wild type FVIII light chain (Table 2). In addition to interaction studies by capturing FVIII light chain variants directly from medium via the C2 domain on an SPR chip, interaction studies were performed using purified FVIII light chain variants and full-length LRP1 (Fig. 7). These studies showed that, although the FVIII light chain variant carrying 5 lysine to arginine replacements demonstrated a 20-fold reduced interaction with LRP1 cluster II, binding to full-length LRP1 was not affected. However, replacements at the same position by alanine or glutamic acid did result in a reduced interaction with full-length LRP1 (Fig. 7).

TABLE 2

Effect of combining lysine replacements on the interaction between the FVIII light chain and LRP1 cluster II

Association and dissociation of LRP1 cluster II to FVIII light chain variants carrying replacements at positions Lys-1693, Lys-1827, and Lys-1967 (A3), Lys-2065 and Lys-2092 (C1), and Lys-1693, Lys-1827, Lys-1967, Lys-2065, and Lys-2092 (A3C1) was assessed by SPR analysis employing a BIAcore 3000 biosensor (Biacore AB, Uppsala, Sweden). The anti-C2 antibody CLB-EL14 IgG4 (26 fmol/mm^{-2}) was immobilized onto a CM5 sensor chip using the amine coupling method according to the manufacturer's instructions. Subsequently, FVIII light chain variants were bound to the anti-C2 antibody at a density of 17 fmol/mm^{-2}. LRP1 cluster II (0.2–200 nM) was passed over the FVIII light chain variants in a buffer containing 150 mM NaCl, 5 mM $CaCl_2$, 0.005% (v/v) Tween 20, and 20 mM Hepes (pH 7.4) at 25 °C with a flow rate of 20 μl/min. The sensor chip surface was regenerated three times after each concentration of LRP1 cluster II using the same buffer containing 1 M NaCl. Binding to FVIII light chain variants was corrected for binding in absence of FVIII. Binding data during the association phase were fitted in a one-phase exponential association model.

	Replacement		
Domain	Arginine (K_D)	Alanine (K_D)	Glutamic acid (K_D)
	nM	nM	nM
A3	201 ± 18	222 ± 20	ND
C1	220 ± 21	620 ± 59	534 ± 52
A3C1	567 ± 48	1339 ± 144	ND

Binding of FVIIIdB Variants to LRP1 Cluster II and Full-length LRP1 from Light Chain to Heterodimer—To verify the contribution of the 5 lysine residues in the FVIII cofactor, we purified FVIIIdB variants carrying 5 lysine to arginine, alanine, or glutamic acid replacements. FVIII variants were bound via the C2 domain to antibody CLB-EL14 IgG4, and a concentration range of LRP1 cluster II was passed over the immobilized FVIII variants. These SPR binding studies indicated that all FVIIIdB variants showed a dramatically reduced interaction with LRP1 cluster II in the order wild type > 5×KR > 5×KA > 5×KE (Fig. 8). Although for individual lysine residues, there was only a minor difference between KR, KA, and KE variants, the combined KE replacements proved to be more detrimental for the interaction with LRP1 cluster II than KA and KR replacements. In addition, we studied the contribution of the 5 lysine residues in the interaction with full-length LRP1. Therefore, we directly coupled full-length LRP1 on the CM5 chip and passed over the FVIIIdB variants. Binding studies indicated that the binding was reduced in the order 5×KR > 5×KA > 5×KE. The binding defect of the

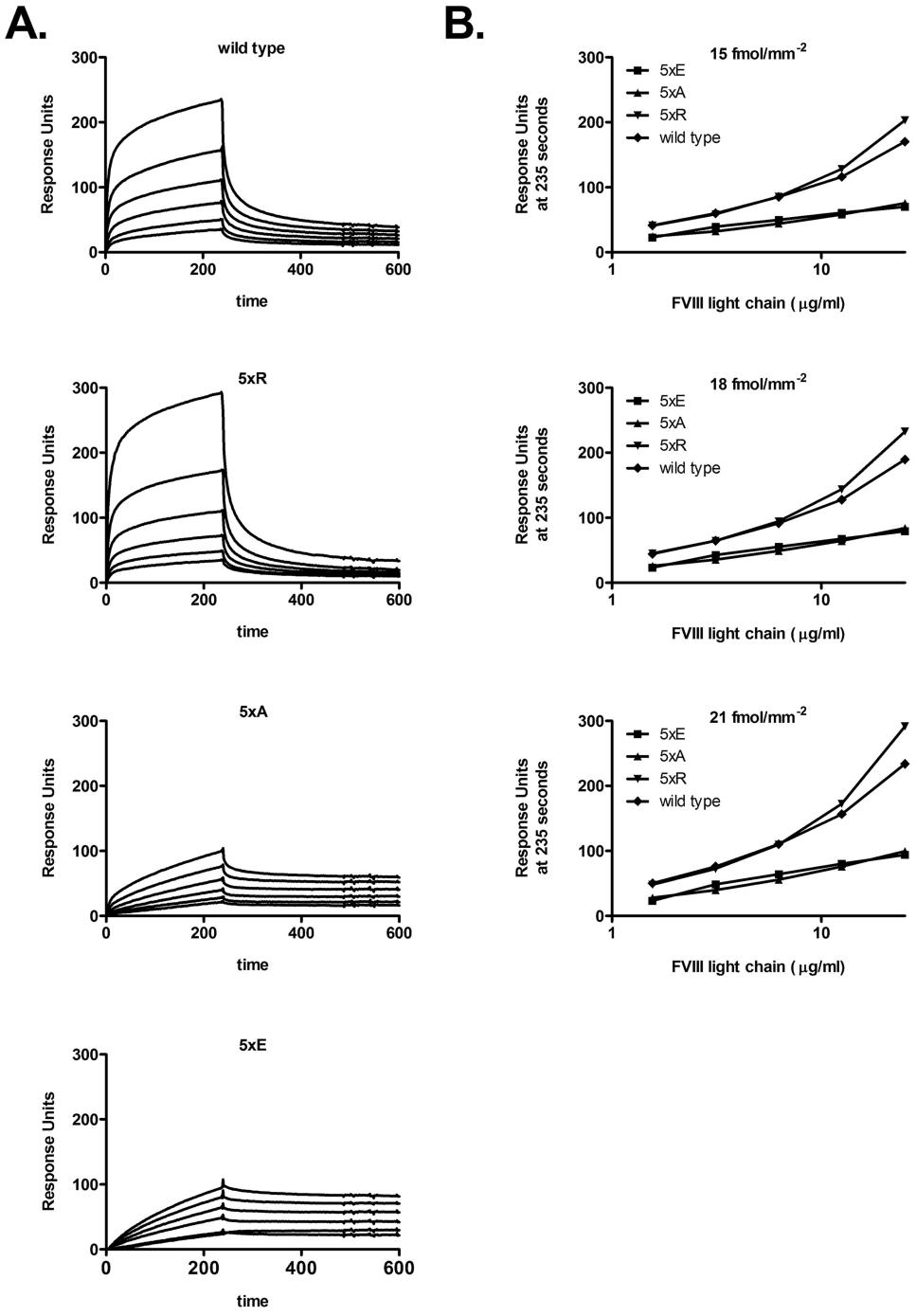

FIGURE 7. **Binding of FVIII light chain variants to full-length LRP1.** *A*, association and dissociation of FVIII light chain variants to full-length LRP1 were assessed by SPR analysis employing a BIAcore 3000 biosensor (Biacore AB). LRP1 (Biomac) was coupled directly on a CM5 chip according to the manufacturer's instructions at three different densities (15, 18, and 21 fmol/mm^{-2}). FVIII light chain variants (1–25 μg/ml based on Bradford analysis) were passed over the immobilized LRP1 in a buffer containing 150 mM NaCl, 5 mM $CaCl_2$, 0.005% (v/v) Tween 20, and 20 mM Hepes (pH 7.4) at 25 °C with a flow rate of 20 μl/min. The sensor chip surface was regenerated three times after each concentration of FVIII using the same buffer containing 1 M NaCl. Binding to LRP1 was corrected for binding in the absence of LRP1. Shown are the SPR curves for the channel on which 21 fmol/mm^{-2} LRP1 was coupled. *B*, The response units at time point 235 s were plotted as a function of the concentration for all three LRP1 surface densities.

5×KR variant was remarkably minor, whereas the binding defects of the 5×KA and 5×KE were more severe (Fig. 9).

Discussion

This study demonstrates that lysine residues indeed make a dominant contribution to the LRP1-FVIII interaction. When we chemically modified all surface-exposed lysine residues of FVIII using NHS-biotin or NHS-sulfo acetate, the binding to LRP1 cluster II is completely abrogated. Our combined experimental approach using HDX-MS and site-directed mutagenesis further suggests that the interaction of LRP1 with FVIII occurs over an extended surface containing multiple lysine residues in FVIII. Hydrogen deuterium exchange-mass spectrometry (HDX-MS) experiments identified regions 114–132, 369–

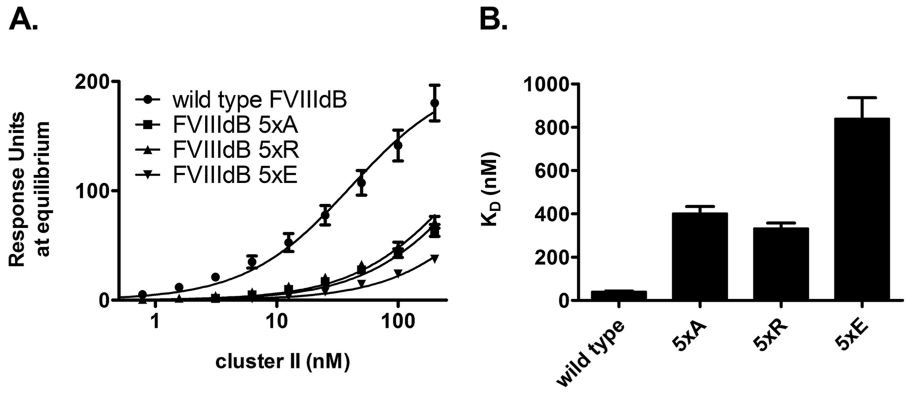

FIGURE 8. **Binding of FVIIIdB variants to LRP1 cluster II.** *A*, association and dissociation of LRP1 cluster II to FVIIIdB variants were assessed by SPR analysis employing a BIAcore 3000 biosensor (Biacore AB). The anti-C2 antibody CLB-EL14 IgG4 (39 fmol/mm^{-2} for FVIIIdB variants) was immobilized onto a CM5 sensor chip using the amine coupling method according to the manufacturer's instructions. Subsequently, FVIIIdB variants were bound to the anti-C2 antibody at a density of 9 fmol/mm^{-2}. LRP1 cluster II (0–200 nM) was passed over the FVIIIdB variants in a buffer containing 150 mM NaCl, 5 mM $CaCl_2$, 0.005% (v/v) Tween 20, and 20 mM Hepes (pH 7.4) at 25 °C with a flow rate of 20 μl/min. The sensor chip surface was regenerated three times after each concentration of LRP1 cluster II using the same buffer containing 1 M NaCl. Binding to FVIIIdB variants was corrected for binding in the absence of FVIII. Binding data during the association phase were fitted in a one-phase exponential association model. *B*, the responses at equilibrium were fitted by non-linear regression using a standard hyperbola to generate K_D values (GraphPad Prism 4 software). *Error bars* indicate ± S.D.

387, 399–428, 481–506, 1669–1689, 1735–1746, 1817–1834, 2054–2069, 2078–2097, 2213–2234, 2264–2273, and 2292–2296 to be involved in the binding of FVIII to LRP1 cluster II. As expected (45), these regions are mainly located in the FVIII light chain and scattered throughout the *a3*, A3, C1, and C2 domains of FVIII. Subsequent SPR analysis of a library of FVIII light chain variants carrying lysine to arginine revealed that multiple (11) lysine residues within the FVIII light chain including 1673/1674, 1693, 1813/1818, 1827, 1967, 1972, 2065, 2092, and 2136 contribute to the interaction with LRP1 cluster II. However, none of the individual lysine residues accounts completely for LRP1 cluster II binding. We did observe an additive effect of combining multiple lysine replacements, and further mutagenesis studies using positively charged arginine, uncharged alanine, or negatively charged glutamic acid residues indicated that reversing the positive charge had the strongest effect on the interaction.

The majority of the lysine residues that were identified in the mutagenesis study are located within those regions that were also identified using the HDX-MS study and are therefore considered "hot spots." These include 1673/1674, 1813/1818, 1827, 2065, and 2092 in FVIII. These data are in good agreement with previously described interactive sites on FVIII that mediate the binding to LRP1 (21, 35) and are fully compatible with our previous observation that the A3C1 domains of FVIII harbor important interaction sites for LRP1 (45). Taken together, the pattern that emerges suggests that ligand binding to LRP1 is supported by a variety of target binding sites that most likely interact simultaneously with multiple CR repeats. The interaction of each individual site may be weak; however, when many interaction sites are in play at the same time, dissociation of a single site will not allow abrogation of the complex. Hence, the combination of many weak binding sites results in an overall strong interaction, suggesting an additive model of interaction. This may explain our observations that the binding defects of both FVIII light chain and FVIIIdB variants containing 5×R replacements for full-length LRP1 were remarkably minor as compared with LRP1 cluster II. In contrast, the binding defects of the FVIII light chain and FVIIIdB variants containing 5×A and 5×E replacements were comparable between LRP1 cluster II and LRP1.

The question remains why certain lysine residues contribute more to the interaction than others. Based on a study on the specificity of binding of the serpins PAI-1 and PN-1 to LRP1, Jensen *et al.* (30) have suggested that there may be modest requirements to be a coordinating lysine residue. However, inspection of the x-ray structure of the LDLR-RAP complex suggests that members of the LDL receptor family interact with clusters of lysines being 18–20 Å apart (12). In addition, it has been suggested that hydrophobic interactions may play an additional role in the binding of ligands to the complement-type repeats (14). Although the acidic necklace model as proposed by Fisher *et al.* (12) suggests that hydrophobic interactions are mediated by the side chain of the lysine residue of the ligand, Jensen *et al.* (14) propose that an additional hydrophobic residue of the ligand, typically a leucine or an isoleucine, is important for the interaction. Therefore, hydrophobic residues located in the vicinity of the lysine residue may determine whether a lysine residue is a hot spot or not. Alternatively, the presence of a second proximal charge near the lysine residue, or perhaps even repulsive charges from amino acid residues surrounding the lysine residue, may determine specificity (17, 29).

No consensus for either hydrophobic or charged residues in the vicinity of our identified lysine residues could be identified. We therefore took a close look at the spatial distribution of the identified interactive regions and lysine residues within FVIII. Crystal structure analysis revealed that all hot-spot lysine residues that we identified may spatially align with the acidic binding pockets of the extracellular part of the LDL receptor. The distance from the bottom of the C1 domain to the top of the A3 domain spans 69 Å, a distance that LRP1 cluster II can easily encompass using just 3–4 complement-type repeats. We therefore propose that LRP1 cluster II interacts with the FVIII light chain via an extended surface that starts at the bottom of the C1 domain and extends to the top of the A3 domain. This prompted us to perform structural modeling with the goal to

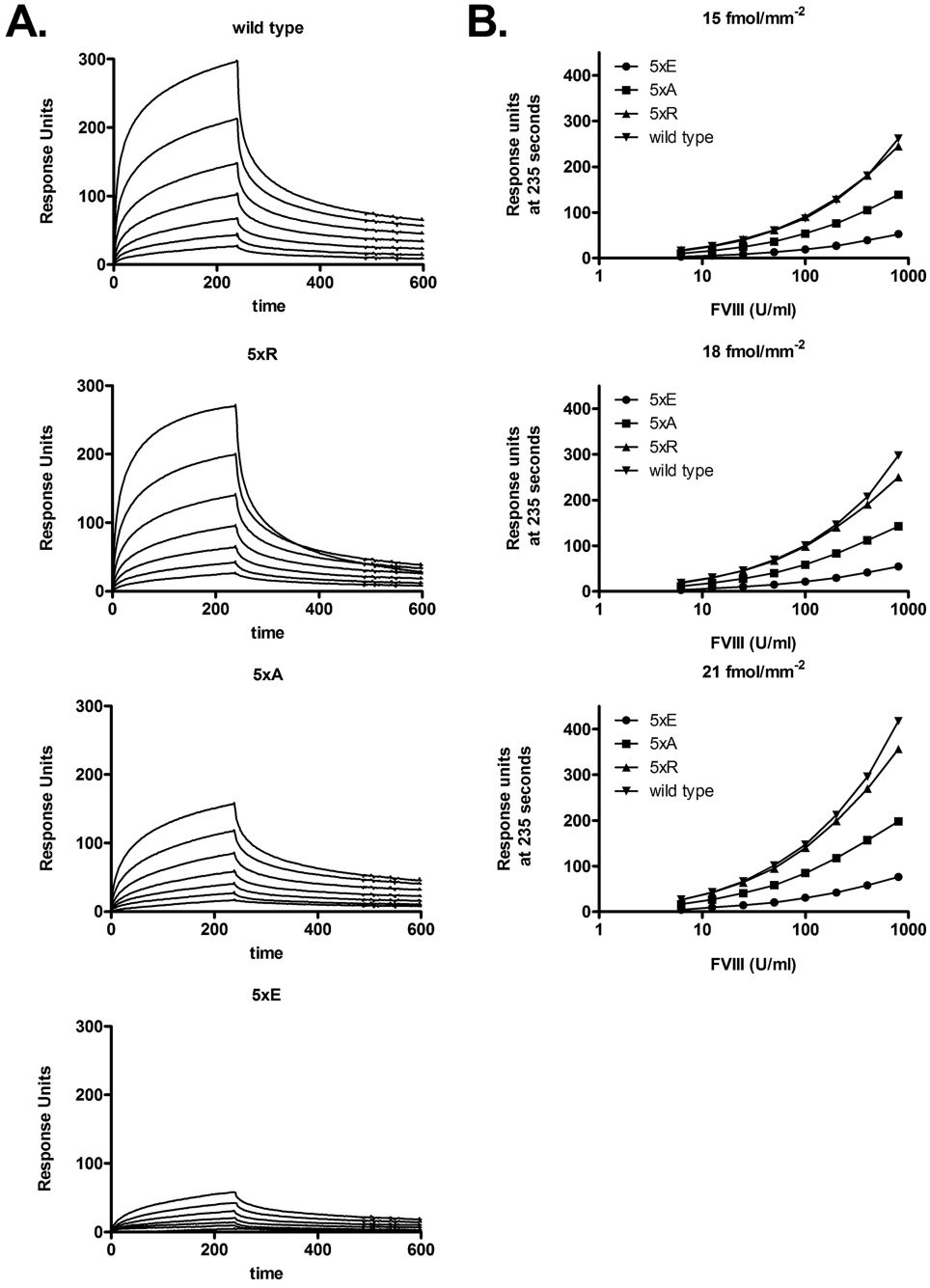

FIGURE 9. **Binding of FVIIIdB variants to full-length LRP1.** *A*, association and dissociation of FVIIIdB variants to full-length LRP1 were assessed by SPR analysis employing a BIAcore 3000 biosensor (Biacore AB). LRP1 (Biomac) was coupled directly on a CM5 chip according to the manufacturer's instructions at three different densities (15, 18, and 21 fmol/mm^{-2}). FVIIIdB variants (5–1000 units/ml based on chromogenic activity) were passed over the immobilized LRP1 in a buffer containing 150 mM NaCl, 5 mM $CaCl_2$, 0.005% (v/v) Tween 20, and 20 mM Hepes (pH 7.4) at 25 °C with a flow rate of 20 μl/min. The sensor chip surface was regenerated three times after each concentration of FVIII using the same buffer containing 1 M NaCl. Binding to LRP1 was corrected for binding in the absence of LRP1. Shown are the SPR curves for the channel on which 21 fmol/mm^{-2} LRP1 was coupled. *B*, the response units at time point 235 s were plotted as a function of the concentration for all three LRP1 surface densities.

both exemplify and substantiate likely interactions between LRP1 cluster II and the FVIII light chain. Initially, we focused on the FVIII C1 domain in which both HDX-MS and mutagenesis studies indicated the contribution of 2 lysine residues in the C1 domain, Lys^{2065} and Lys^{2092}. Homology modeling was performed in consensus with the canonical binding mode for members of the LDL receptor family using the x-ray crystallographic structure of the LDLR-RAP complex as a template (12) (Fig. 10). Hence, each CR module contains three acidic aspartic acid residues placed in a concave surface region that interacts with lysine clusters. The proposed canonical interaction mode between LRP1 triple module and the FVIII light chain allows two principal binding modes oppositely oriented relative to each other, *i.e.* LRP1 N terminus to C terminus aligns along the Lys^{2065}-Lys^{2092}-Lys^{2136} as opposed to Lys^{2136}-Lys^{2092}-Lys^{2065} surface patch. Two key features contribute to a favorable interaction between lysine regions and the LRP triple module. Shape complementarity is eminently achievable due to the flexible

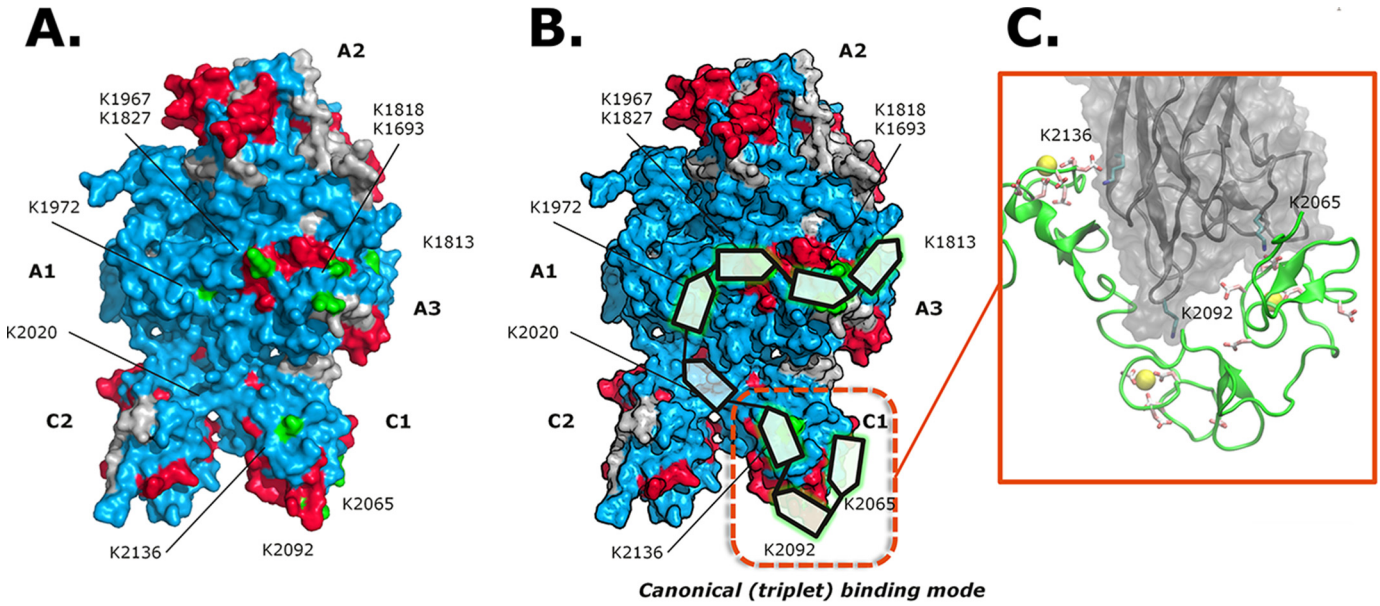

FIGURE 10. **Model for FVIII-LRP1 interaction.** *A*, surface plot of FVIII based on the crystal structure (Protein Data Bank code 4BDV) with peptides showing a reduced HDX exchange in *red*, with peptides showing an unaltered HDX exchange in *blue*, and with interacting lysine residues in *green*. *B*, schematic representation of the suggested LRP1 cluster II interaction (8 complement-type repeats represented in *green*) with the FVIII light chain. *C*, the canonical (triplet) mode is emphasized (*red square*), and the binding motif between the calcium-loaded LRP triple module (*green*) and FVIII C1 (*gray*) is represented by a graphic. Aspartic acid residues of LRP and the hot-spot lysine residues of FVIII are shown as sticks.

nature of the chain of complementary repeats, allowing the receptor to adapt to the ligands' surface topology and exploit hydrophobic interaction in between repeats. Also, the ionic interactions between the positively charged lysine residues and the negatively charged aspartic acid residues resulted in close packing of the partners, suggesting that these features are the driving forces behind the interaction. The widespread imprint of LRP1 binding on FVIII identified by HDX-MS analysis points to the notion that during LRP1 binding, CR repeats switch between different lysine clusters. This is reflected in the designed LRP1 model where several interacting modes are equally likely (Fig. 10).

In addition to the overlap of HDX and the lysine mutagenesis study, there were also some differences. Residues 1693, 1967, 1972, and 2136 were identified only in the lysine mutagenesis study, whereas regions 1735–1746, 2213–2234, 2264–2273, and 2292–2296 were only identified using the HDX-MS approach. We therefore consider these regions and lysine residues "soft spots." The effect of the soft-spot lysine residues may be explained by conformational changes; lysine residue 1693 is directly facing the hot-spot lysine at position 1818, and the soft-spot lysine residue 1967 has been shown to interact with the A2 domain of FVIII (46). As for the soft-spot regions identified by HDX-MS, region 1735–1746 is located within the A3 region and consists of the amino acids FQEFTDGSFTQP. The remaining 3 regions are located within the C2 domain. The C2 domain has previously been reported to bind to LRP1 with low affinity ($K_D \approx 3.6\ \mu M$) (45). The region 2292–2296 (PVVNS) contains no positively charged residues, the region 2264–2273 (SSQDGHQWTL) contains 1 histidine residue, and the region 2213–2234 (QGRSNAWRPQVNNPKEWLQVDF) contains 2 arginine residues and 1 lysine residue. We did not observe any contribution of lysine residues in the C2 domain of FVIII to the interaction with LRP1 in our mutagenesis study (Fig. 4*E*), suggesting that the reported low affinity of the C2 domain may be mediated by residues other than lysine.

In recent years, the importance of the C domains in the life cycle of FVIII has been appreciated because they are involved in lipid binding, von Willebrand factor (VWF) interaction, and cellular uptake (47–52). The C2 domain is loosely attached to the C1 and A1 domains, and it is likely that the domain has a high degree of rotational freedom. We believe that the positioning of the FVIII C domains relative to each other may therefore be an important aspect in the biology of FVIII. The regions in the C2 domain that were identified by HDX-MS may reflect conformational changes within these areas as opposed to a direct interaction with LRP1 cluster II. The dynamics of the FVIII C domains in response to interaction with various ligands and lipids remains a subject for further studies.

Acknowledgment—We thank Dr. Helle Heibroch Petersen for production of LRP cluster II for the HDX-MS studies.

REFERENCES

1. Herz, J., Chen, Y., Masiulis, I., and Zhou, L. (2009) Expanding functions of lipoprotein receptors. *J. Lipid Res.* **50,** S287–S292
2. Krieger, M., and Herz, J. (1994) Structures and functions of multiligand lipoprotein receptors: macrophage scavenger receptors and LDL receptor-related protein (LRP). *Annu. Rev. Biochem.* **63,** 601–637
3. Dieckmann, M., Dietrich, M. F., and Herz, J. (2010) Lipoprotein receptors: an evolutionarily ancient multifunctional receptor family. *Biol. Chem.* **391,** 1341–1363
4. Herz, J., and Strickland, D. K. (2001) LRP: a multifunctional scavenger and signaling receptor. *J. Clin. Invest.* **108,** 779–784
5. Strickland, D. K., and Ranganathan, S. (2003) Diverse role of LDL receptor-related protein in the clearance of proteases and in signaling. *J. Thromb. Haemost.* **1,** 1663–1670
6. Fass, D., Blacklow, S., Kim, P. S., and Berger, J. M. (1997) Molecular basis of familial hypercholesterolaemia from structure of LDL receptor module.

Nature **388,** 691–693
7. Andersen, O. M., Christensen, L. L., Christensen, P. A., Sørensen, E. S., Jacobsen, C., Moestrup, S. K., Etzerodt, M., and Thogersen, H. C. (2000) Identification of the minimal functional unit in the low density lipoprotein receptor-related protein for binding the receptor-associated protein (RAP): a conserved acidic residue in the complement-type repeats is important for recognition of RAP. *J. Biol. Chem.* **275,** 21017–21024
8. Brown, M. S., Herz, J., and Goldstein, J. L. (1997) LDL-receptor structure: calcium cages, acid baths and recycling receptors. *Nature* **388,** 629–630
9. Moestrup, S. K., Kaltoft, K., Sottrup-Jensen, L., and Gliemann, J. (1990) The human α_2-macroglobulin receptor contains high affinity calcium binding sites important for receptor conformation and ligand recognition. *J. Biol. Chem.* **265,** 12623–12628
10. Strickland, D. K., Ashcom, J. D., Williams, S., Battey, F., Behre, E., McTigue, K., Battey, J. F., and Argraves, W. S. (1991) Primary structure of α_2-macroglobulin receptor-associated protein: human homologue of a Heymann nephritis antigen. *J. Biol. Chem.* **266,** 13364–13369
11. Herz, J., Goldstein, J. L., Strickland, D. K., Ho, Y. K., and Brown, M. S. (1991) 39-kDa protein modulates binding of ligands to low density lipoprotein receptor-related protein/α_2-macroglobulin receptor. *J. Biol. Chem.* **266,** 21232–21238
12. Fisher, C., Beglova, N., and Blacklow, S. C. (2006) Structure of an LDLR-RAP complex reveals a general mode for ligand recognition by lipoprotein receptors. *Mol. Cell* **22,** 277–283
13. Migliorini, M. M., Behre, E. H., Brew, S., Ingham, K. C., and Strickland, D. K. (2003) Allosteric modulation of ligand binding to low density lipoprotein receptor-related protein by the receptor-associated protein requires critical lysine residues within its carboxyl-terminal domain. *J. Biol. Chem.* **278,** 17986–17992
14. Jensen, G. A., Andersen, O. M., Bonvin, A. M., Bjerrum-Bohr, I., Etzerodt, M., Thøgersen, H. C., O'Shea, C., Poulsen, F. M., and Kragelund, B. B. (2006) Binding site structure of one LRP-RAP complex: implications for a common ligand-receptor binding motif. *J. Mol. Biol.* **362,** 700–716
15. van den Biggelaar, M., Sellink, E., Klein Gebbinck, J. W., Mertens, K., and Meijer, A. B. (2011) A single lysine of the two-lysine recognition motif of the D3 domain of receptor-associated protein is sufficient to mediate endocytosis by low-density lipoprotein receptor-related protein. *Int. J. Biochem. Cell Biol.* **43,** 431–440
16. Zaiou, M., Arnold, K. S., Newhouse, Y. M., Innerarity, T. L., Weisgraber, K. H., Segall, M. L., Phillips, M. C., and Lund-Katz, S. (2000) Apolipoprotein E-low density lipoprotein receptor interaction: influences of basic residue and amphipathic α-helix organization in the ligand. *J. Lipid Res.* **41,** 1087–1095
17. Dolmer, K., Campos, A., and Gettins, P. G. (2013) Quantitative dissection of the binding contributions of ligand lysines of the receptor-associated protein (RAP) to the low density lipoprotein receptor-related protein (LRP1). *J. Biol. Chem.* **288,** 24081–24090
18. Bu, G., Geuze, H. J., Strous, G. J., and Schwartz, A. L. (1995) 39 kDa receptor-associated protein is an ER resident protein and molecular chaperone for LDL receptor-related protein. *EMBO J.* **14,** 2269–2280
19. Willnow, T. E., Armstrong, S. A., Hammer, R. E., and Herz, J. (1995) Functional expression of low density lipoprotein receptor-related protein is controlled by receptor-associated protein *in vivo*. *Proc. Natl. Acad. Sci. U.S.A.* **92,** 4537–4541
20. Willnow, T. E., Rohlmann, A., Horton, J., Otani, H., Braun, J. R., Hammer, R. E., and Herz, J. (1996) RAP, a specialized chaperone, prevents ligand-induced ER retention and degradation of LDL receptor-related endocytic receptors. *EMBO J.* **15,** 2632–2639
21. Meems, H., van den Biggelaar, M., Rondaij, M., van der Zwaan, C., Mertens, K., and Meijer, A. B. (2011) C1 domain residues Lys 2092 and Phe 2093 are of major importance for the endocytic uptake of coagulation factor VIII. *Int. J. Biochem. Cell Biol.* **43,** 1114–1121
22. Howard, G. C., Yamaguchi, Y., Misra, U. K., Gawdi, G., Nelsen, A., DeCamp, D. L., and Pizzo, S. V. (1996) Selective mutations in cloned and expressed α-macroglobulin receptor binding fragment alter binding to either the α_2-macroglobulin signaling receptor or the low density lipoprotein receptor-related protein/α_2-macroglobulin receptor. *J. Biol. Chem.* **271,** 14105–14111
23. Lalazar, A., Weisgraber, K. H., Rall, S. C., Jr., Giladi, H., Innerarity, T. L., Levanon, A. Z., Boyles, J. K., Amit, B., Gorecki, M., Mahley, R. W., *et al.* (1988) Site-specific mutagenesis of human apolipoprotein E: receptor binding activity of variants with single amino acid substitutions. *J. Biol. Chem.* **263,** 3542–3545
24. Nielsen, K. L., Holtet, T. L., Etzerodt, M., Moestrup, S. K., Gliemann, J., Sottrup-Jensen, L., and Thogersen, H. C. (1996) Identification of residues in α-macroglobulins important for binding to the α_2-macroglobulin receptor/low density lipoprotein receptor-related protein. *J. Biol. Chem.* **271,** 12909–12912
25. Rodenburg, K. W., Kjoller, L., Petersen, H. H., and Andreasen, P. A. (1998) Binding of urokinase-type plasminogen activator-plasminogen activator inhibitor-1 complex to the endocytosis receptors α_2-macroglobulin receptor/low-density lipoprotein receptor-related protein and very-low-density lipoprotein receptor involves basic residues in the inhibitor. *Biochem. J.* **329,** 55–63
26. Stefansson, S., Muhammad, S., Cheng, X. F., Battey, F. D., Strickland, D. K., and Lawrence, D. A. (1998) Plasminogen activator inhibitor-1 contains a cryptic high affinity binding site for the low density lipoprotein receptor-related protein. *J. Biol. Chem.* **273,** 6358–6366
27. Williams, S. E., Inoue, I., Tran, H., Fry, G. L., Pladet, M. W., Iverius, P. H., Lalouel, J. M., Chappell, D. A., and Strickland, D. K. (1994) The carboxyl-terminal domain of lipoprotein lipase binds to the low density lipoprotein receptor-related protein/α_2-macroglobulin receptor (LRP) and mediates binding of normal very low density lipoproteins to LRP. *J. Biol. Chem.* **269,** 8653–8658
28. Lee, C. J., De Biasio, A., and Beglova, N. (2010) Mode of interaction between β2GPI and lipoprotein receptors suggests mutually exclusive binding of β2GPI to the receptors and anionic phospholipids. *Structure* **18,** 366–376
29. Gettins, P. G., and Dolmer, K. (2012) A proximal pair of positive charges provides the dominant ligand-binding contribution to complement-like domains from the LRP (low-density lipoprotein receptor-related protein). *Biochem. J.* **443,** 65–73
30. Jensen, J. K., Dolmer, K., and Gettins, P. G. (2009) Specificity of binding of the low density lipoprotein receptor-related protein to different conformational states of the clade E serpins plasminogen activator inhibitor-1 and proteinase nexin-1. *J. Biol. Chem.* **284,** 17989–17997
31. van den Biggelaar, M., Bierings, R., Storm, G., Voorberg, J., and Mertens, K. (2007) Requirements for cellular co-trafficking of factor VIII and von Willebrand factor to Weibel-Palade bodies. *J. Thromb Haemost.* **5,** 2235–2242
32. van den Biggelaar, M., Meijer, A. B., Voorberg, J., and Mertens, K. (2009) Intracellular cotrafficking of factor VIII and von Willebrand factor type 2N variants to storage organelles. *Blood* **113,** 3102–3109
33. Thim, L., Vandahl, B., Karlsson, J., Klausen, N. K., Pedersen, J., Krogh, T. N., Kjalke, M., Petersen, J. M., Johnsen, L. B., Bolt, G., Nørby, P. L., and Steenstrup, T. D. (2010) Purification and characterization of a new recombinant factor VIII (N8). *Haemophilia* **16,** 349–359
34. Fribourg, C., Meijer, A. B., and Mertens, K. (2006) The interface between the EGF2 domain and the protease domain in blood coagulation factor IX contributes to factor VIII binding and factor X activation. *Biochemistry* **45,** 10777–10785
35. Bovenschen, N., Boertjes, R. C., van Stempvoort, G., Voorberg, J., Lenting, P.J.,Meijer,A.B.,andMertens,K.(2003)Lowdensitylipoproteinreceptor-related protein and factor IXa share structural requirements for binding to the A3 domain of coagulation factor VIII. *J. Biol. Chem.* **278,** 9370–9377
36. Andersen M.D., and Faber J. H. (2011) Structural characterization of both the non-proteolytic and proteolytic activation pathways of coagulation Factor XIII studied by hydrogen-deuterium exchange mass spectrometry. *Int. J. Mass Spectrom.* **302,** 139–148
37. Kavan, D., and Man, P. (2011) MSTools: Web based application for visualization and presentation of HXMS data. *Int. J. Mass Spectrom.* **302,** 53–58
38. van Helden, P. M., van den Berg, H. M., Gouw, S. C., Kaijen, P. H., Zuurveld, M. G., Mauser-Bunschoten, E. P., Aalberse, R. C., Vidarsson, G., and Voorberg, J. (2008) IgG subclasses of anti-FVIII antibodies during immune tolerance induction in patients with hemophilia A. *Br. J. Haematol.*

142, 644–652
39. Leyte, A., Mertens, K., Distel, B., Evers, R. F., De Keyzer-Nellen, M. J., Groenen-Van Dooren, M. M., De Bruin, J., Pannekoek, H., Van Mourik, J. A., and Verbeet, M. P. (1989) Inhibition of human coagulation factor VIII by monoclonal antibodies: mapping of functional epitopes with the use of recombinant factor VIII fragments. *Biochem. J.* **263,** 187–194
40. Leaver-Fay, A., Tyka, M., Lewis, S. M., Lange, O. F., Thompson, J., Jacak, R., Kaufman, K., Renfrew, P. D., Smith, C. A., Sheffler, W., Davis, I. W., Cooper, S., Treuille, A., Mandell, D. J., Richter, F., Ban, Y. E., Fleishman, S. J., Corn, J. E., Kim, D. E., Lyskov, S., Berrondo, M., Mentzer, S., Popović, Z., Havranek, J. J., Karanicolas, J., Das, R., Meiler, J., Kortemme, T., Gray, J. J., Kuhlman, B., Baker, D., and Bradley, P. (2011) ROSETTA3: an object-oriented software suite for the simulation and design of macromolecules. *Methods Enzymol.* **487,** 545–574
41. Phillips, J. C., Braun, R., Wang, W., Gumbart, J., Tajkhorshid, E., Villa, E., Chipot, C., Skeel, R. D., Kalé, L., and Schulten, K. (2005) Scalable molecular dynamics with NAMD. *J. Comput. Chem.* **26,** 1781–1802
42. Chivian, D., and Baker, D. (2006) Homology modeling using parametric alignment ensemble generation with consensus and energy-based model selection. *Nucleic Acids Res.* **34,** e112
43. Svensson, L. A., Thim, L., Olsen, O. H., and Nicolaisen, E. M. (2013) Evaluation of the metal binding sites in a recombinant coagulation factor VIII identifies two sites with unique metal binding properties. *Biol. Chem.* **394,** 761–765
44. Ebina, T., Toh, H., and Kuroda, Y. (2009) Loop-length-dependent SVM prediction of domain linkers for high-throughput structural proteomics. *Biopolymers* **92,** 1–8
45. Lenting, P. J., Neels, J. G., van den Berg, B. M., Clijsters, P. P., Meijerman, D. W., Pannekoek, H., van Mourik, J. A., Mertens, K., and van Zonneveld, A. J. (1999) The light chain of factor VIII comprises a binding site for low density lipoprotein receptor-related protein. *J. Biol. Chem.* **274,** 23734–23739
46. Bloem, E., Meems, H., van den Biggelaar, M., van der Zwaan, C., Mertens, K., and Meijer, A. B. (2012) Mass spectrometry-assisted study reveals that lysine residues 1967 and 1968 have opposite contribution to stability of activated factor VIII. *J. Biol. Chem.* **287,** 5775–5783
47. Gilbert, G. E., Novakovic, V. A., Kaufman, R. J., Miao, H., and Pipe, S. W. (2012) Conservative mutations in the C2 domains of factor VIII and factor V alter phospholipid binding and cofactor activity. *Blood* **120,** 1923–1932
48. Meems, H., Meijer, A. B., Cullinan, D. B., Mertens, K., and Gilbert, G. E. (2009) Factor VIII C1 domain residues Lys 2092 and Phe 2093 contribute to membrane binding and cofactor activity. *Blood* **114,** 3938–3946
49. Gilbert, G. E., Kaufman, R. J., Arena, A. A., Miao, H., and Pipe, S. W. (2002) Four hydrophobic amino acids of the factor VIII C2 domain are constituents of both the membrane-binding and von Willebrand factor-binding motifs. *J. Biol. Chem.* **277,** 6374–6381
50. Lü, J., Pipe, S. W., Miao, H., Jacquemin, M., and Gilbert, G. E. (2011) A membrane-interactive surface on the factor VIII C1 domain cooperates with the C2 domain for cofactor function. *Blood* **117,** 3181–3189
51. Bloem, E., van den Biggelaar, M., Wroblewska, A., Voorberg, J., Faber, J. H., Kjalke, M., Stennicke, H. R., Mertens, K., and Meijer, A. B. (2013) Factor VIII C1 domain spikes 2092–2093 and 2158–2159 comprise regions that modulate cofactor function and cellular uptake. *J. Biol. Chem.* **288,** 29670–29679
52. Herczenik, E., van Haren, S. D., Wroblewska, A., Kaijen, P., van den Biggelaar, M., Meijer, A. B., Martinez-Pomares, L., ten Brinke, A., and Voorberg, J. (2012) Uptake of blood coagulation factor VIII by dendritic cells is mediated via its C1 domain. *J. Allergy Clin. Immunol* **129,** 501–509

Protein Structure and Folding:

Factor VIII Interacts with the Endocytic Receptor Low-density Lipoprotein Receptor-related Protein 1 via an Extended Surface Comprising ''Hot-Spot'' Lysine Residues

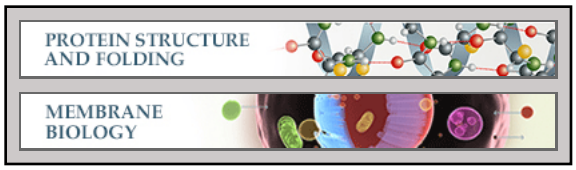

Maartje van den Biggelaar, Jesper J. Madsen, Johan H. Faber, Marleen G. Zuurveld, Carmen van der Zwaan, Ole H. Olsen, Henning R. Stennicke, Koen Mertens and Alexander B. Meijer

J. Biol. Chem. 2015, 290:16463-16476.
doi: 10.1074/jbc.M115.650911 originally published online April 21, 2015
